

Cite this: *Polym. Chem.*, 2026, **17**, 946

Structure–melt viscosity relationship of discrete sequence-specific linear oligo(dimethylsiloxane-co-diphenylsiloxane)s

Hiroyuki Minamikawa, * Takahiro Kawatsu  and Kazuhiro Matsumoto *

Polysiloxanes are widely used in various household, industrial, and biomedical products; however, the effects of their composition and sequence on the melt viscosity have not been investigated in detail. A series of discrete linear oligosiloxanes with precisely controlled compositions and sequences was prepared in this study, and the relationship between their molecular structures and melt viscosities was examined. The oligomers possessed linear structures composed of dimethylsiloxo (**D**) and diphenylsiloxo (**P**) units with trimethylsiloxy (**M**) ends. **P**-repeat oligomers contained consecutive **P** blocks including exact numbers of **P** units. The prepared oligomers were employed to explore the specific effects of block structures. The 26-meric sequence isomers exhibited identical **M/D/P** compositions and four sequence-repeating blocks: (**PD**)₁₂, (**PPDD**)₆, (**PPPPDD**)₄, and (**PPPPDDDD**)₃. This facile synthetic methodology enabled the preparation of well-defined oligomers on the gram scale and estimation of their melt viscosities through actual measurements. The oligodimethylsiloxanes were also compared using previously reported viscosity values. Each oligosiloxane was uniform in terms of the **M/D/P** composition, sequence, and molecular weight. These oligosiloxanes were distinguished by their viscosity–molecular weight relationships; a steep enhancement in viscosity with an increasing number of consecutively repeated **P** units and a distinct influence of block sequence patterns on the viscosity of the 26-mers were observed. To gain molecular insights, the oligosiloxane viscosities were analyzed using the Rouse model and its modifications, and the effects of structural factors on the melt viscosity of the oligosiloxanes were discussed. The findings of this work demonstrate that appropriate Rouse model variants can effectively explain how the composition and sequence influence the melt viscosity of oligosiloxanes.

Received 7th October 2025,
Accepted 30th January 2026

DOI: 10.1039/d5py00958h

rsc.li/polymers

1 Introduction

Siloxanes are widely utilized in personal care, household, industrial, and biomedical products.^{1–3} Taking various physical forms, such as oils, greases, waxes, rubbers, and resins, oligodimethylsiloxanes and polydimethylsiloxanes (PDMS) have been formulated into lubricants, antifoams, mold releases, adhesives, coatings, sealants, thermal and electrical insulators, and contact lens materials. Notably, attaching phenyl substituents to silicon atoms in PDMS drastically changes the macroscopic properties of the resulting copolymers. While PDMS undergoes crystallization between –50 and –40 °C according to its heating thermograms, the crystallization process is completely suppressed after 4–6 mol% substitution with methylphenylsiloxane⁴ and diphenylsiloxane^{5,6} in

PDMS chains. For poly(dimethylsiloxane-co-diphenylsiloxane), substitution in the 6–60 mol% range monotonically elevates the glass transition temperature^{5,7,8} and enhances the thermal stability.⁸ These structural effects are usually described in terms of the average molecular weight, content, and sequence.^{4–13}

Siloxane copolymers with phenyl substitution have been prepared *via* the condensation of silanolates and chlorosilanes,^{5,9} condensation of alkoxy silanes and hydro silanes (the Piers–Rubinsztajn reaction),¹¹ ring-opening polymerization of cyclotrisiloxanes,^{4–6,8,10,12–14} and convergent preparation of block copolymers.¹⁵ In these polymerization reactions, random copolymerization to a phenyl content of 64 mol%⁸ and preparation of strictly alternating poly(dimethyl-co-diphenylsiloxane)⁹ and phenyl-rich block copolymers¹¹ have been reported. Nevertheless, the fine control of the copolymer structure remains a difficult task. The copolymers inherently exhibit distributions of molecular weights, phenyl substitution contents, and sequence. Additionally, preparing diverse sequence patterns during polymerization is

Research Institute for Chemical Process Technology, National Institute of Advanced Industrial Science and Technology (AIST), Tsukuba Central 5, 1-1-1 Higashi, Tsukuba, Ibaraki 305-8565, Japan. E-mail: hiroyuki.minamikawa@aist.go.jp, kazuhiro.matsumoto@aist.go.jp



ing the Rouse model^{29,30,32} and its modifications and discussed the effect of structural factors on the melt viscosity.

2 Results and discussion

2.1 Sequence-controlled preparation of linear oligo (dimethylsiloxane-co-diphenylsiloxane)s

Discrete P-repeat oligomers 2–6 with 3–8 consecutive P units were successfully prepared following the synthetic methodology described in ref. 18. Notably, four or more consecutive P units are practically inaccessible as pure compounds by conventional methods. The 26-meric siloxane oligomers 7–10 possessing specific block sequences were prepared using the method described in ref. 19.

2.2 Viscosity measurements

Viscosity measurements showed that oligomers 2–10 in the melt were viscous liquids. For each oligosiloxane, the shear viscosity η was nearly constant below the shear rate $\dot{\gamma}$ of 100 s^{-1} (Fig. S1). We utilized the viscosity at $\dot{\gamma} = 10 \text{ s}^{-1}$ as the zero-shear viscosity η_0 .

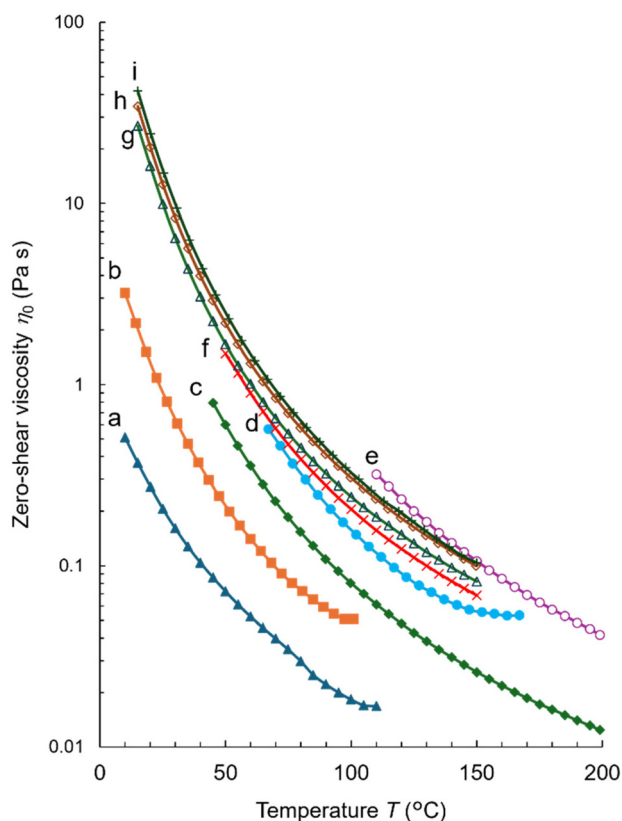


Fig. 2 Zero-shear viscosities η_0 of the liquid siloxane oligomers plotted as functions of temperature T (shear rate $\dot{\gamma} = 10 \text{ s}^{-1}$). P-repeat oligomers: (a) 2 (blue filled triangles, \blacktriangle), (b) 3 (orange filled squares, \blacksquare), (c) 4 (green filled diamonds, \blacklozenge), (d) 5 (light blue filled circles, \bullet), and (e) 6 (purple open circles, \circ). 26-mers: (f) 7 (red crosses, \times), (g) 8 (green open triangles, Δ), (h) 9 (brown open diamonds, \diamond), and (i) 10 (green pluses, $+$). The curves f–i are redrawn from ref. 19.

Fig. 2 shows the zero-shear viscosities η_0 of the liquid siloxane oligomers plotted as functions of temperature T . The viscosity of each melt yields a separate curve, which monotonously decreases with temperature. Among the P-repeat oligomers 2–6, the temperature–viscosity curves are uniformly shifted upwards in the sequence $2 < 3 < 4 < 5 < 6$ (curves a–e) for 3–8 consecutive P units. For the 26-meric sequence isomers 7–10, the curves are shifted upwards in the sequence $7 < 8 < 9 < 10$ (curves f–i).

Fig. 3 compares the zero-shear viscosities η_0 of the oligosiloxanes at 70 and 110 °C plotted as functions of molecular weight M . Here, the molecular weights are precise and not average values. For the dimethylsiloxane oligomers, the viscosity values are taken from the literature.^{21,22} The plot distinguishes three types of oligomers using the $\eta_0 - M$ power law relationship. In a series of dimethylsiloxane oligomers 1_n (filled squares), the relationships $\eta_0 \sim M^{1.4}$ and $\eta_0 \sim M^{1.3}$ can be observed at 70 and 110 °C (the black lines), respectively, and the exponents are typical ones for oligomeric compounds.^{28–30}

At the above-mentioned temperatures, the viscosities of the P-repeat oligomers 2–6 (open circles) were between 0.01 and 1 Pa s, which were as large as those of PDMS with molecular weights above 10^4 g mol^{-1} . Moreover, the viscosities steeply increased with M as $\eta_0 \sim M^{4.8}$ at 70 °C and $\eta_0 \sim M^{4.0}$ at 110 °C (the orange lines). It is a striking observation because the exponents of 4.0 and 4.8 obtained for the oligomers are exceptionally large as compared with the values of 3.2–3.6 determined for the previously reported entangled polymers.^{28–30,33–35} These results revealed that the consecutive P-repeats exhibited highly cumulative viscosity enhancements.

The viscosity values of 7–10 at 70 and 110 °C are plotted as the open triangles in Fig. 3. Despite the identical composition and molecular weight ($3431.7 \text{ g mol}^{-1}$), these isomers exhibit relatively small but distinct differences in viscosity, as mentioned previously.¹⁹ More specifically, their viscosities increased in the sequence $7 < 8 < 9 < 10$ in the measured temperature range of 50–150 °C (Fig. 2). At each temperature, 10 produced 1.5–1.7 times higher viscosities than isomer 7; the observed differences were significant during viscosity measurements. These results demonstrate that the sequence patterns strongly influence the melt viscosity of the isomers.

In this section, the zero-shear viscosities of the oligosiloxanes with precise structures were compared. Their viscosity was significantly influenced by structural factors such as molecular weight, composition, and sequence. In particular, our precise synthesis allowed measuring and comparing the viscosities of P-repeat oligomers and 26-mers to demonstrate that the obtained values were highly sensitive to the compositions and sequences of the P and D groups. In section 2.3, we analyze these measurement results using a discrete Rouse model and its modifications.

2.3 Rouse model estimation

We examined the 7 to 12-mers 2–6 and the 26-meric isomers 7–10. Being significantly shorter than entangled PDMS chains (465-mers or longer),²⁷ the chains were analyzed as unentangled ones. The viscosity of oligosiloxane liquids is sensitive



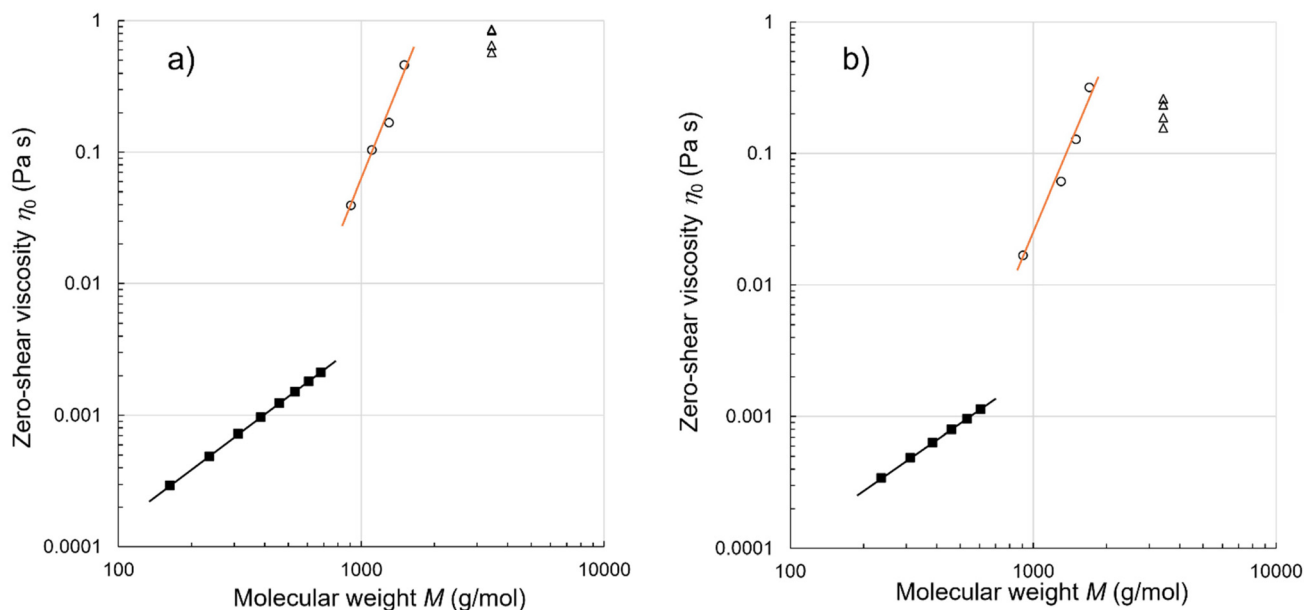


Fig. 3 Zero-shear viscosities η_0 of the siloxane oligomers plotted as functions of molecular weight M . (a) 1_n (filled squares, \blacksquare , $n = 2-9$), 2 , 3 , 4 , and 5 (open circles, \circ), and 7 , 8 , 9 , and 10 (open triangles, Δ) at $70\text{ }^\circ\text{C}$. (b) 1_n (filled squares, \blacksquare , $n = 3-8$), 2 , 4 , 5 , and 6 (open circles, \circ), and 7 , 8 , 9 , and 10 (open triangles, Δ) at $110\text{ }^\circ\text{C}$. The following lines are eye guides: (a) $\eta_0 \sim M^{1.4}$ (black) and $\eta_0 \sim M^{4.8}$ (orange); and (b) $\eta_0 \sim M^{1.3}$ (black) and $\eta_0 \sim M^{4.0}$ (orange).

to the **M/D/P** composition and sequence as well as to their molecular weight. In this section, the viscosities are estimated using four models: the Rouse model³² and its modifications, Models A, B, and C. In these bead-spring models, **M**, **D**, and **P** units are treated as beads that cause intermolecular friction, and Si–O–Si linkages are considered harmonic spring bonds relaxing to equilibration lengths. The specific sequence of each oligosiloxane is represented in a matrix with one-to-one correspondence. Throughout this study, the matrices were processed in a discrete form without transforming the bead-spring structure into a continuous, smooth string object. The discrete Rouse model³⁶ provides a direct and effective method for analyzing the fine effects of defined sequences (details of the calculation procedure are described in the SI). The model parameters and measured and estimated viscosities are listed in Tables S1–S4.

For the oligodimethylsiloxanes 1_n , the density values were taken from ref. 20–22. In estimating the oligomer viscosities, the parameters σ_M and σ_D were optimized. For the **P**-containing oligomers 2–10, we assumed a molecular volume as the sum of the included unit volumes. From the specific volume of the **MPM** trimer, denoted as **MD**M*** in ref. 20, the **P** unit volume was estimated by interpolation at $70\text{ }^\circ\text{C}$ and by extrapolation at $110\text{ }^\circ\text{C}$.

2.3.1 Discrete Rouse model and Model A. In a series of dimethylsiloxane oligomers 1_n , the discrete Rouse model was successfully applied to estimate their viscosities. The results obtained at 70 and $110\text{ }^\circ\text{C}$ are shown in Fig. S2. After optimizing the parameters σ_M and σ_D for the **M** and **D** units, the obtained estimates were in good agreement with the relation-

ships $\eta_0 \sim M^{1.4}$ at $70\text{ }^\circ\text{C}$ and $\eta_0 \sim M^{1.3}$ at $110\text{ }^\circ\text{C}$, which represented typical behavior of unentangled oligomers. Fig. 4a and 5a show the model estimates for the **P**-repeat oligomers 2, 3, 4, and 5 at $70\text{ }^\circ\text{C}$ and 2, 4, 5, and 6 at $110\text{ }^\circ\text{C}$, respectively. The extraordinarily steep slopes (the dashed lines) in the plots were not reproduced by the optimization of σ_P in the original form of the Rouse model (plotted as x). This result encouraged us to modify the model for the consecutive **P**-repeats, which causes a cumulative increase in viscosity.

To discuss the observed effects of the **P**-consecutive blocks, we here take intermolecular π – π or CH– π interaction into consideration. **P** units can interact intermolecularly with each other through relatively weak interactions, but the pair may easily dissociate. For the **P**-consecutive blocks, however, the dissociated **P** unit can find another **P** unit nearby in the counterpart block and immediately associate. Hence, the block structures may effectively prolong the original intermolecular pair, especially for the long **P**-consecutive blocks. This picture is speculative but may suggest some aspects of the observed increase in melt viscosity. It should also be noted that the reassociation process between associating units can play a critical role in the rheological behavior of weakly associative copolymers.³⁷ We should check the plausible picture by simulation in the future.

In general, the larger friction coefficients result in longer relaxation times, leading to higher viscosity. To figure out the cumulative effect of the **P**-consecutive blocks in the matrix-based formulation, Model A introduces a phenomenological parameter (<1). To reproduce the observed exponential increase in viscosity for the **P**-consecutive oligomers, we replaced the matrix com-



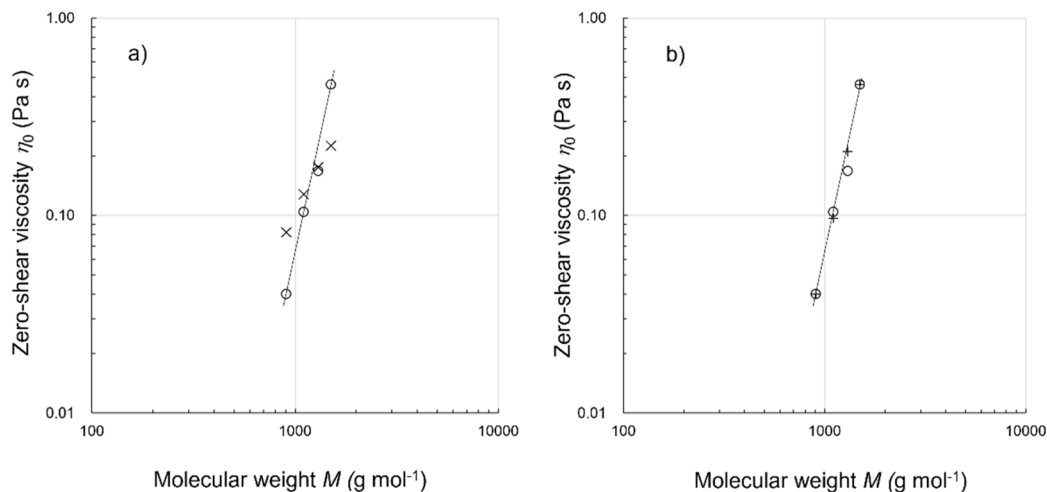


Fig. 4 The viscosities of the P-repeat oligomers 2, 3, 4, and 5 at 70 °C as a function of molecular weight M . \circ , the measured values; \times , discrete Rouse model estimation (a); and $+$, Model A estimation (b). The lines are eye-guides for $\eta_0 \sim M^{4.8}$.

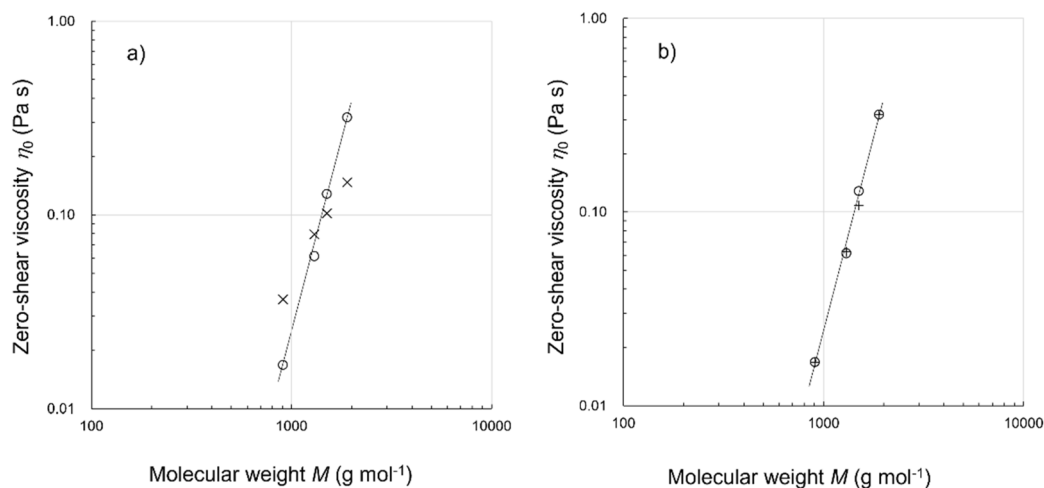


Fig. 5 The viscosities of the P-repeat oligomers 2, 4, 5, and 6 at 110 °C as a function of molecular weight M . \circ , the measured values; \times , discrete Rouse model estimation (a); and $+$, Model A estimation (b). The lines are eye guides for $\eta_0 \sim M^{4.0}$.

ponents σ_p with $\alpha^n \sigma_p$. It has been found that the factors α^n increase the viscosity estimates in an exponential manner. Taking PPPPPP for instance, the series $\alpha \sigma_p$, $\alpha^2 \sigma_p$, $\alpha^3 \sigma_p$, $\alpha^4 \sigma_p$, $\alpha^5 \sigma_p$, and $\alpha \sigma_p$ did not give the observed steep increase in viscosity; in contrast, the series $\alpha \sigma_p$, $\alpha^2 \sigma_p$, $\alpha^3 \sigma_p$, $\alpha^4 \sigma_p$, $\alpha^5 \sigma_p$, and $\alpha \sigma_p$ successfully reproduced the observation. Parameters σ_M and σ_D were taken from the 1_n estimation described above. The model details are provided in the SI.

Fig. 4b and 5b show the Model A estimations for the P-repeat oligomers 2, 3, 4, and 5 at 70 °C and 2, 4, 5, and 6 at 110 °C, respectively. The estimation (+) strongly agreed with the measured relations $\eta_0 \sim M^{4.8}$ at 70 °C and $\eta_0 \sim M^{4.0}$ at 110 °C. This model functioned effectively for the P-repeat oligomers.

Fig. 6a compares the logarithmic values of the measured viscosities at 70 °C and Model A estimations. The dashed line

is an eye guide. From left to right, the open circles indicate the P-repeat oligomers 2, 3, 4, and 5, and the open triangles denote the 26-mers 7, 8, 9, and 10. For the four P-repeat oligomers and 26-mers 9 and 10, the plots are located on the line. In contrast, the estimates obtained for 7 and 8 are significantly lower than the measured values. The coefficient of determination in Fig. 6a is 0.902. Model A was not sufficiently accurate for oligomers 7 and 8, which contained the repeating blocks of PD and PPDD, respectively. In the next section, we discuss Model B to improve our estimation accuracy.

2.3.2 Model B. The Rouse model and Model A assume flexible chains, in which bond directions are random and independent of the neighboring or closely located bonds. Variants of the Rouse model have been proposed to simulate semiflexible chains using bond–bond correlations (local chain rigidity).^{38–42} In Model B, bond–bond correlations are intro-



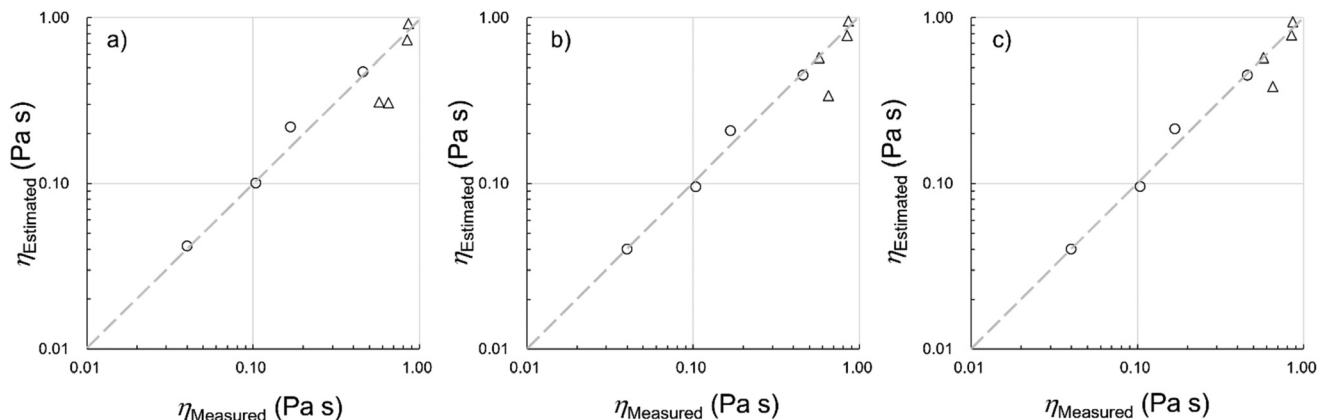


Fig. 6 The measured and estimated viscosities at 70 °C of P-repeat siloxane oligomers 2, 3, 4, and 5 (○) and 26-mers 7, 8, 9, and 10 (Δ). (a) Model A estimation. (b) Model B estimation. (c) Model C estimation. The dashed lines are eye guides.

duced for oligosiloxanes. Focusing on the **PPP**, **PPD**, and **PDP** sequences in the studied oligomers, we used three bond–bond correlation parameters: e , f , and g , respectively. Model estimations and a plausible mechanism of local chain rigidity are described in the SI.

Fig. 6b compares the Model B estimations with the measurement data obtained at 70 °C. The estimations for 7 and 8 are particularly improved using this model. The plot constructed for the eight oligosiloxanes yields a coefficient of determination of 0.948. These results demonstrate that the bond–bond correlation or local chain rigidity can strongly influence the chain relaxation responsible for liquid viscosity.

In Model B, the effects produced by the consecutive **P** units and local chain rigidity are simultaneously examined. When parameter α was set to 1 (no enhancement by the consecutive **P** units), the optimization resulted in a value of e equal to unity, reflecting the perfect rigidity in the **PPP** sequence. However, the estimated exponent in the $\eta_0 - M$ relationship for the consecutive **P** oligomers was 3.4 for 2–5 at 70 °C and 3.2 for 2–6 at 110 °C, which were considerably lower than the experimental values (4.8 at 70 °C and 4.0 at 110 °C). The α values of 0.183 at 70 °C and 0.301 at 110 °C, along with a zero e value, produced the estimates that were in good agreement with the measurement results (Fig. 6b and Fig. S5b, Table S1). This result indicates that a small α value works effectively not only for reproducing the consecutive **P**-sequence enhancement but also for expressing the **PPP** chain rigidity in place of e . Meanwhile, the estimated non-zero f and g values effectively improved the viscosity estimations for the 26-mers 7–10.

2.3.3 Model C. The above-mentioned models simply assume common friction coefficients ζ_M , ζ_D , and ζ_P for different oligomers. Model C employs the friction coefficients $\tilde{\zeta}_M$, $\tilde{\zeta}_D$, and $\tilde{\zeta}_P$, which vary with the oligomer composition. First, the area fractions of **M**, **D**, and **P** units were estimated for each oligosiloxane. Second, the friction coefficients $\tilde{\zeta}_M$, $\tilde{\zeta}_D$, and $\tilde{\zeta}_P$ were calculated from the area fractions. Finally, a semi-flexible chain estimation was performed using a procedure similar to that used in Model B (computational details are pro-

vided in the SI). Fig. 6c shows the Model C estimations obtained for the **P**-repeat isomers and 26-mers at 70 °C. Some improvements were achieved in the estimation for 8, as indicated by its higher coefficient of determination equal to 0.962.

2.3.4 Temperature effects on model estimations. This section discusses several effects of temperature on model estimations. Fig. S3–S5 show the results obtained for the **P**-repeat oligomers and 26-mers at 85, 100, and 110 °C. (i) At 70 °C (Fig. 6) and 85 °C (Fig. S2), Model B demonstrated estimation improvements, especially for the two 26-mers 7 and 8. The bond–bond correlation can be a critical factor in analyzing the structure–property relationships of siloxanes with various block patterns. (ii) At 100 °C (Fig. S4) and 110 °C (Fig. S5), the Model A estimations were in better agreement with the measurement data than the estimations obtained at 70 and 85 °C. At higher temperatures, polymer chains may be considered flexible to a certain extent. (iii) These figures show that Model C agrees well with the measurement results. In the Model C estimations, the coefficients of determination were as high as 0.962 (70 °C) and 0.990 (110 °C).

The present models only consider the relaxation modes of Si–O–Si bond stretching of linear siloxane chains. For branched or cyclic siloxane structures, we should develop relaxation-based models with bending or ring flipping modes.

3 Conclusions

In the present work, we synthesized discrete sequence-specific oligosiloxanes 2–10 containing **M**, **D**, and **P** units. Using our synthetic methodology, we successfully prepared oligosiloxanes with precise molecular weights, **M/P/D** compositions, and sequences on the gram scale. This efficient preparation procedure allowed us to investigate the effects of structural factors on the melt viscosity. In particular, we observed a steep enhancement in viscosity by the consecutive **P** repeats and a distinct influence of the block sequence patterns on the viscosity of the 26-mers.



We applied the Rouse model and its modifications to estimate the viscosities of the sequence-specific oligomers synthesized in this work and oligodimethylsiloxanes reported in the literature. Representing the specific sequences with matrices, Model A successfully simulated the cumulative viscosity enhancement in the successive P-repeat blocks. This model is useful for applications involving P-repeat siloxanes. By considering bond–bond correlations (local chain rigidity), Model B improved the viscosity estimations for the 26-mers. The semiflexible chain approach particularly improved the estimates for the oligosiloxanes with PPD and PDP sequences. Model C considered the friction coefficients to be composition-dependent and further increased the estimation accuracy. This study demonstrates that appropriate Rouse model variants can effectively explain how the composition and sequence influence the melt viscosity of oligosiloxanes.

The gram-scale synthesis procedure employed in the present work can be used to prepare different types of discrete sequence-specific siloxanes possessing various sequence patterns, cyclic or branched topologies, and other functionalities.^{16–18} These varieties include telechelic oligosiloxanes with definite functionalities, which exhibit a high application potential in functional copolymerization.⁴³ In addition, further characterization of these oligosiloxanes will be beneficial for elucidating the influence of siloxane structures on their physicochemical properties and designing and developing siloxanes for future applications. For discrete sequence-specific oligosiloxanes, our group is currently studying their structure–property relationships by investigating phase transitions, thermal stability, miscibility, and single-crystal properties, as well as their applications as novel materials.

Author contributions

T. K. and K. M. conducted the design and synthesis of oligosiloxanes. H. M. carried out shear viscosity measurement and analysis. H. M. and K. M. discussed the results and wrote the manuscript.

Conflicts of interest

There are no conflicts to declare.

Data availability

The data supporting this article have been included as part of the supplementary information (SI). Supplementary information is available. See DOI: <https://doi.org/10.1039/d5py00958h>.

Acknowledgements

This work was supported by JST PRESTO (Grant Number: JPMJPR21AE), Japan. The authors thank Ms Mariko Okada for her help in the preparation of siloxane materials.

References

- R. G. Jones, W. Ando and J. Chojnowski, *Silicon-Containing Polymers*, Kluwer Academic Publishers, Dordrecht, the Netherlands, 2000.
- M. A. Brook, *Silicon in Organic, Organometallic, and Polymer Chemistry*, John Wiley, New York, 2000.
- S. J. Clarson, M. J. Owen, S. D. Smith and M. E. Van Dyke, *Advances in Silicones and Silicone-Modified Materials*, ACS Publication, Washington, D. C., 2010.
- A. Zlatanic, D. Radojcic, X. Wan, J. M. Messman, D. E. Bowen and P. R. Dvornic, *J. Polym. Sci., Part A: Polym. Chem.*, 2019, **57**, 1122.
- G. N. Babu, S. S. Christopher and R. A. Newmark, *Macromolecules*, 1987, **20**, 2654.
- A. Zlatanic, D. Radojcic, X. Wan, J. M. Messman and P. R. Dvornic, *Macromolecules*, 2017, **50**, 3532.
- I. Yilgör and J. E. MacGrath, *Adv. Polym. Sci.*, 1988, **86**, 1.
- J. Shi, N. Zhao, S. Xia, S. Liu and Z. Li, *Polym. Chem.*, 2019, **10**, 2126.
- K.-A. T. Nguyen, S. R. Clarke, J. Matisons, B. W. Skelton, A. H. White and E. Markovic, *Silicon*, 2014, **6**, 21.
- L. Zhu, X. Cheng, W. Su, J. Zhao and C. Zhou, *Polymers*, 2019, **11**, 1989.
- A. F. Schneider, E. K. Lu, G. Lu and M. A. Brook, *J. Polym. Sci.*, 2020, **58**, 3095.
- Y. Yu, Y. Zhao, B. Huang, Y. Li, Y. Zhao, Z. Zhang and H.-F. Fei, *Polymer*, 2022, **249**, 124865.
- S. Wang, Z. Peng, Y. Huang, M. Zhu, Y. Liu and Y. Zhang, *Polymer*, 2024, **311**, 127554.
- B. R. Harkness, M. Tachikawa, H. Yu and I. Mita, *Chem. Mater.*, 1998, **10**, 1700.
- T. M. Gädda and W. P. Weber, *J. Polym. Sci., Part A: Polym. Chem.*, 2006, **44**, 3629.
- K. Matsumoto, Y. Oba, Y. Nakajima, S. Shimada and K. Sato, *Angew. Chem., Int. Ed.*, 2018, **57**, 4637.
- K. Matsumoto, S. Shimada and K. Sato, *Chem. – Eur. J.*, 2019, **25**, 920.
- T. Kawatsu, J.-C. Choi, K. Sato and K. Matsumoto, *Macromol. Rapid Commun.*, 2021, **42**, 20000593.
- T. Kawatsu, H. Minamikawa, K. Sato and K. Matsumoto, *Polym. Chem.*, 2024, **15**, 2740.
- C. B. Hurd, *J. Am. Chem. Soc.*, 1946, **68**, 364.
- D. F. Wilcock, *J. Am. Chem. Soc.*, 1946, **68**, 691.
- E. B. Baker, A. J. Barry and M. J. Hunter, *Ind. Eng. Chem.*, 1946, **38**, 1117.
- A. J. Barry, *J. Appl. Phys.*, 1946, **17**, 1020.
- H. I. Waterman, W. E. R. van Herwijnen and H. W. den Hartog, *J. Appl. Chem.*, 1958, **8**, 62.



- 25 T. G. Fox and V. R. Allen, *J. Chem. Phys.*, 1964, **41**, 344.
- 26 T. Kataoka and S. Ueda, *J. Polym. Sci., Part B: Polym. Lett.*, 1966, **4**, 317.
- 27 P. R. Dvornic, J. D. Jovanovic and M. N. Govedarica, *J. Appl. Polym. Sci.*, 1993, **49**, 1497.
- 28 G. C. Berry and T. G. Fox, *Adv. Polym. Sci.*, 1968, **5**, 261.
- 29 M. Doi and S. F. Edwards, *The Theory of Polymer Dynamics*, Clarendon Press, Oxford, 1986.
- 30 G. Strobl, *The Physics of Polymers*, Springer, Berlin Heidelberg New York, 2007.
- 31 S. M. Aharoni, *Macromolecules*, 1983, **16**, 1722.
- 32 P. E. Rouse, *J. Chem. Phys.*, 1953, **21**, 1272.
- 33 A. Casale, R. S. Porter and J. F. Johnson, *J. Macromol. Sci., Part C: Polym. Rev.*, 1971, **5**, 387.
- 34 M. Abdel-Goad, W. Pyckhout-Hintzen, S. Kahle, J. Allgaier, D. Richter and L. J. Fetters, *Macromolecules*, 2004, **37**, 8135.
- 35 L. Yang, T. Uneyama, Y. Masubuchi and Y. Doi, *J. Soc. Rheol., Jpn.*, 2021, **49**, 267.
- 36 G. Tsolou, N. Stratikis, C. Baig, P. S. Stephanou and V. G. Marvranzas, *Macromolecules*, 2010, **43**, 10692. The discrete model is presented in the Appendix.
- 37 X. Cui, Y. Luo, Y. Yang and P. Tang, *Macromolecules*, 2025, **58**, 1898.
- 38 M. Bixon and R. Zwanzig, *J. Chem. Phys.*, 1978, **68**, 1896.
- 39 R. G. Winkler, P. Reineker and L. Harnau, *J. Chem. Phys.*, 1994, **101**, 811.
- 40 M. G. Guenza, *J. Phys.: Condens. Matter*, 2008, **20**, 033101.
- 41 M. Dolgushev and A. Blumen, *Macromolecules*, 2009, **42**, 5378.
- 42 A. R. Tejedor, J. R. Tejedor and J. Ramírez, *J. Chem. Phys.*, 2022, **157**, 164904.
- 43 E. Yilgör and I. Yilgör, *Prog. Polym. Sci.*, 2014, **39**, 1165.

